

RSC Advances



This is an *Accepted Manuscript*, which has been through the Royal Society of Chemistry peer review process and has been accepted for publication.

Accepted Manuscripts are published online shortly after acceptance, before technical editing, formatting and proof reading. Using this free service, authors can make their results available to the community, in citable form, before we publish the edited article. This *Accepted Manuscript* will be replaced by the edited, formatted and paginated article as soon as this is available.

You can find more information about *Accepted Manuscripts* in the [Information for Authors](#).

Please note that technical editing may introduce minor changes to the text and/or graphics, which may alter content. The journal's standard [Terms & Conditions](#) and the [Ethical guidelines](#) still apply. In no event shall the Royal Society of Chemistry be held responsible for any errors or omissions in this *Accepted Manuscript* or any consequences arising from the use of any information it contains.

Apigenin mediated gold nanoparticle synthesis and their anti-cancer effect on human epidermoid carcinoma (A431) cells

Indra Rajendran^a, Harini Dhandapani^a, Rajaram Anantanarayanan^b, Rama Rajaram^{*a}

^a, * Department of Biochemistry, Central Leather Research Institute, Adyar, India

^b Department of Biophysics, Central Leather Research Institute, Adyar, India

*Corresponding Author

Dr. Rama Rajaram

Biochemistry Laboratory

Central Leather Research Institute

Adyar, Chennai - 600 020

India

Email: rajaram.rama@gmail.com

Tel: +91-44-24437177

Abstract

We report that the flavonoid, apigenin (4', 5, 7,-trihydroxyflavone) is able to form apigenin linked gold nanoparticles (ap-AuNPs) at RT with apigenin itself acting as the stabilizing agent. The synthesized ap-AuNPs have been characterised by UV- Visible spectroscopy, HR-TEM, DLS, FTIR and TGA analyses. The biocompatible nature of ap-AuNPs is shown by its non - toxicity towards normal epidermoid cells (HaCat). Additionally, it is shown to exhibit anti-cancer activity towards epidermoid squamous carcinoma cells (A431). The uptake of ap-AuNPs into A431 cells is seen by TEM. Apoptosis induced by ap-AuNPs in these cells is observed through EtBr/AO and DAPI staining. Flow cytometric results also reveal the occurrence of early apoptotic cells, late apoptotic cells and the presence of sub-G1 population. DNA prepared from ap-AuNPs treated A-431 cells reveals a ladder like pattern in agarose gel electrophoresis indicating oligonucleosomal cleavage which is a hallmark of apoptosis. The ap-AuNPs also inhibit angiogenesis as shown by Chick chorioallantoic membrane (CAM) assay. Taking the results together, we believe that ap-AuNPs show promise in treatment of skin cancer. The ap-AuNPs also have cytotoxic potential against the human cervical squamous cell carcinoma cell line - SiHa.

Keywords: Apigenin; AuNPs; A431 cells; HaCat cells; SiHa; Anti-carcinogenicity; Chorioallantoic membrane

Introduction

The incidence of skin cancer has been increasing during the last decade.¹ Overexposure to solar UV radiation and chemicals such as arsenic and nickel are the major etiological factors for the development of malignancy.²⁻⁴ Therefore, there is a need to develop novel therapeutic agents which preferably target cancer cells leaving normal cells unaffected. Gold nanoparticles (AuNPs) have attracted considerable attention due to their possible applications in cancer treatment, in drug delivery, as biosensors, in photo thermal therapy and in imaging.⁵⁻¹⁰ AuNPs have been synthesized by reducing Au³⁺ ions employing chemical reductants such as citrate, CTAB, etc., and the shape and size of the particles are tunable by adjusting the conditions employed.¹¹⁻¹³ Applications in biomedicine are however limited when the capping and stabilizing agents used have toxic effects in biological systems.^{11,13} For example, citrate reduced AuNPs are found to be toxic towards normal human dermal microvascular endothelial cells (HDMEC) and human cerebral microvascular endothelial cells (hCMEC).¹³ The synthesis of AuNPs using plant extracts and phytochemicals may prove advantageous over the AuNPs made via chemical capping.¹⁴⁻¹⁶ Phytochemicals like (-) epigallocatechin-3-gallate (EGCG), resveratrol, tannins etc, have all been used for forming colloidal gold from ionic solutions of gold.¹⁶⁻¹⁸

The flavones which are one of the secondary metabolites of plants, exhibit antioxidant, antimicrobial, anti-proliferative and anti-carcinogenic properties.^{19, 20} Flavonoids like apigenin, quercetin, genistein etc., have been shown to exhibit anti-cancer activity while being nontoxic to normal cells.²⁰ Some of the flavones that have been shown to reduce Au³⁺ ions to form AuNPs are apiin, dihydromyricetin, quercetin, tannic acid and rutin. The -OH and C=O groups present are reported to aid in the reduction of Au³⁺ and in the stabilization of the AuNPs formed.^{16, 21-24}

Apigenin is a flavonoid (4', 5, 7,-trihydroxyflavone), derived from edible fruits and vegetables including parsley, onions, oranges, tea, chamomile, wheat sprouts and some seasonings.²⁵ It is non-mutagenic and possesses antimicrobial, antiviral and anti-carcinogenic activities.^{26,27} When prostate cancer cells (22Rv1) are exposed to apigenin, enhanced ROS generation, activation of wild-type p53 and induction of apoptosis have been observed.²⁸ Skin carcinoma induced by 12-O-tetradecanoylphorbol-13-acetate (TPA) in mice model has been shown to be inhibited by topical application of 20 $\mu\text{mol/ Kg}$ body weight of apigenin.²⁷ It also inhibits the transcription of vascular endothelial growth factor (VEGF) in ovarian cells and thus inhibits tumour growth and tumour angiogenesis in mice.^{29,30} The concomitant antitumor activity of apigenin and ABT-263 (Bcl-2 inhibitor) is found to be enhanced both *in vitro* and *in vivo* in human colon cancer cells.³¹ Recent reports indicate that apigenin suppresses proliferation and migration and induces apoptosis of T24 bladder cancer cells and breast cancer (T47D and MDA-MB-231) cells.^{32,33} In human skin malignant melanoma (A375) and lung carcinoma cell lines (A549), apigenin induces apoptosis at 80 and 90 $\mu\text{g / mL}$ respectively by modulating the mitochondrial oxidative phosphorylation system.³⁴

The effect of flavonoids is reported to be enhanced when they are in nano-formulations.³⁵ The possible use of flavonoids in the treatment of several cancers also suggest the use of ap-AuNPs in treating skin cancer.^{14, 36} However it is not known whether apigenin can reduce Au^{3+} to form stable gold nanoparticles and if they have any effect on carcinogenic epidermoid cells. Here we report that apigenin conjugated to gold nanoparticles (ap-AuNPs) are formed when apigenin reacts with Au^{3+} under appropriate conditions. The ap-AuNPs are also found to exhibit toxicity towards A431 (epidermoid squamous cell carcinoma) cells while being non-toxic towards

normal epidermoid cells (HaCat). Further, the cytotoxic effect of these ap-AuNPs on another squamous cell line (SiHa) is also demonstrated.

Results and discussion

Synthesis and formation of ap-AuNPs

The formation of ap-AuNPs has been investigated using different molar ratios of apigenin to HAuCl₄ (1: 1 to 1:5) and at different pH values of apigenin (8 - 11). Mixing apigenin and HAuCl₄ solutions at neutral pH do not result in the formation of particles. Formation of ap-AuNPs occurs at RT when the pH of apigenin is increased as observed through the color change from straw yellow to burgundy red. This has also been monitored using a spectrophotometer (Fig. 1). When the pH of apigenin is increased to 8, a small surface plasmon resonance (SPR) peak at 540 nm is observed indicating ap-AuNPs formation, but the particles formed are found to be unstable. As the pH is increased to 9, a new peak at 750 nm is observed in addition to the peak at 540 nm (Fig. 1a). This may indicate the formation of nanoparticles which are of different shapes. Increase in intensity as well as narrowing of the SPR peak at 540 nm is observed when the pH of apigenin is increased to 10 and this generally is a characteristic of monodispersed nanoparticles. Since the pKa value of apigenin as determined by HPLC method is ~ 10 the complete solubility of apigenin at this pH may be leading to the reduction of Au³⁺ to Au⁰ and hence the formation of monodispersed AuNPs.³⁷ On increasing the pH of apigenin to 11, a turbid red coloured colloidal solution is formed and the SPR peak shifts to 560 nm. The particles are also found to settle down indicating that they are unstable. The results indicate that the pH of apigenin solution is crucial for the formation of uniformly sized nanoparticles. The pH dependency of AuNPs formation has also been observed with other flavones like dihydromyricetin and curcumin when they are the reductants.^{22, 38} Since, ap-AuNPs prepared

with apigenin at pH 10 only are found to be monodispersed, further characterisations have been performed on these samples.

In order to optimise the conditions for synthesis, reaction of apigenin with HAuCl_4 at different molar ratios (1:1 to 1:5) has been carried out. On increasing the concentration of HAuCl_4 , the intensity of SPR peak at 540 nm also increases and at a molar ratio of 1:4, it is found to be the maximum (Fig. 1b). When the molar ratio is increased to 1:5, a shift in the SPR peak is observed (590 nm) and the peak is also broad indicating that the particles are not of uniform size. A small and clear shift in SPR towards longer wavelength and decrease in the bandwidth with increasing ratio of apigenin to HAuCl_4 from 1:1 to 1:4 and pH of apigenin from 8 - 10 indicates that uniform particles are formed at the saturating concentrations than at lower concentrations (Fig. S1a and S1b). Thus, a molar ratio of apigenin to HAuCl_4 of 1:4 (0.3 mM of apigenin: 1.2 mM of HAuCl_4) and a pH of apigenin at 10 are found to be the optimum parameters for the synthesis of monodispersed ap-AuNPs. The UV - Visible spectroscopy method has been used as a conventional method for qualitatively determining the yield of AuNPs. A SPR value of around 1.7 obtained for ap-AuNPs (when 1.2 mM of HAuCl_4 is used) indicates that the yield is similar to that of AuNPs formed when citrate is used as the reductant.³⁹

Characterisation of ap-AuNPs

High Resolution -Transmission Electron Microscopy (HR-TEM)

The morphology of the ap-AuNPs has been analysed by HR-TEM. Regular, spherical particles of uniform size having an average diameter of 14.5 ± 3.6 nm are formed at pH 10 (Fig. 2a). A mixture of structures such as triangles, prisms and spheres are obtained with an average size of 29.2 ± 8.0 nm at a pH of 9 (Fig. S2a and S2b). The histogram indicates the narrow size

distribution of the particles at pH 10 while at pH 9 the particles formed have wider size distribution (Fig. 2a and Fig. S.2a inset). These results clearly confirm that the peak in the NIR region corresponds to particles possessing different shapes indicating that apigenin at a pH of 9 is not able to reduce Au^{3+} uniformly. Our results are similar to the reports of Santos et al., 2005, where peaks at NIR region corresponding to different shaped particles were observed in the case of AuNPs reduced with fulvic acid.^{40,41} Fig. 2b shows the lattice planes corresponding to gold over a single nanoparticle. The selected area electron diffraction (SAED) pattern of ap-AuNPs at both pH corresponds to the values (111), (200), (220) and (311), indicating that the ap-AuNPs are crystalline in nature (Fig. 2c & Fig. S2c). AuNPs formed in the presence of morin also possess similar narrow size distribution when the pH is above 9.5.³⁶

X-Ray diffraction analysis (XRD)

The Bragg reflection peaks at $2\Theta = 37^\circ$, 43° and 65° are predominant and can be indexed as (111), (200), (220) and (311) reflections of metallic gold respectively (Fig. 2d). The results corroborate with the standard data (JCPDS file no. 04-0784) confirming the crystalline nature of Au core in the ap-AuNPs.

Dynamic Light Scattering (DLS) and Zeta potential

The hydrodynamic diameter of ap-AuNPs has been determined using dynamic light scattering (DLS) method (Fig. 2e). The average size of ap-AuNPs prepared is found to be 22.2 ± 0.3 nm. A zeta potential value of -32.2 mV indicates that the ap-AuNPs formed are stable (Fig. 2f). No precipitation of particles or changes in the SPR spectrum is observed over a period of 3 months at pH 10 indicating the stability of the ap-AuNPs at RT (Fig. S3).

Fourier transform infrared spectroscopy (FT-IR)

The FTIR spectra of apigenin and ap-AuNPs prepared using apigenin at pH 10 are shown in Fig. 2g. The spectrum of pure apigenin shows a deep band at 3422 cm^{-1} representing the -OH stretch of the phenolic groups at the C⁶-OH and C⁹-OH regions. The absence of this deep peak for ap-AuNPs synthesised at pH 10 suggests that these bonds are possibly involved in the formation of the ap-AuNPs. The band at 1384 cm^{-1} corresponding to the out-of-plane bending vibrations of the C¹⁷-OH group is also absent indicating the involvement of the hydroxyl group in the formation of ap-AuNPs at pH 10. This hydroxyl group is intact in the ap-AuNPs prepared at pH 9 indicating that the particular hydroxyl group is not involved in the formation of ap-AuNPs (Fig. S4). The band 634 cm^{-1} is attributed to the out-of-plane bending vibrations of the phenolic groups. The absence of this band in the ap-AuNPs spectra is evidence for the involvement of the polar groups in the reduction of Au³⁺. The band at 1645 cm^{-1} assigned to the C=O stretching vibrations appear in all the spectra indicating that the keto group remains unaltered at the end of the reaction. The CCC ring vibrations represented by the band at 1020 cm^{-1} and the alkyl ring vibrations associated with the band at 2924 cm^{-1} can be observed in the ap-AuNPs spectra indicating the presence of apigenin on the ap-AuNPs formed.^{42,43} These results show the involvement of the polar hydroxyl groups of apigenin in reducing and capping the ap-AuNPs.

Thermogravimetric analysis (TGA)

The TGA spectrum of ap-AuNPs shows a significant weight loss of apigenin conjugated to the AuNPs (Fig. 2h) with increase in temperature. The thermal decomposition of ap-AuNPs is seen in 3 stages between 30°C and 800°C. The first stage of decomposition from 30°C to 100°C with weight loss of 4% may be due to the escape of water molecules present. The next decomposition process is at around 379°C with weight loss around 8%. The third stage of the decomposition of ap-AuNPs appears at 473°C with weight loss around 13 %. The last stage indicates that apigenin

is conjugated to AuNPs which is degraded under high temperature. The amount of apigenin conjugated to the ap-AuNPs is thus around 21 % and the gold core comprises the remaining. These results are similar to morin reduced AuNPs and quercetin coated citrate reduced AuNPs.^{36,44}

Mechanism of ap-AuNPs formation

Fig. 1c, illustrates the kinetics of the formation of ap-AuNPs when apigenin solution at pH 10 is used for synthesis. During ap-AuNPs formation, initially a broad absorption spectrum is obtained and as the reaction progresses, the SPR centred at 540 nm becomes narrower. Burgundy red coloured ap-AuNPs are obtained within 10-20 min of the reaction, and maximum SPR intensity is obtained after 3 h of reaction. The gradual narrowing of the peak and the uniform spherical particles obtained finally indicate that the nanoparticles might have formed through a process of temporal evolution where large sized particles are first formed which then get cleaved to smaller sized particles.²² The HR-TEM images indicate the presence of monodispersed spherical particles.

At a pH of 9, besides the SPR peak at 540 nm, another peak at 750 nm is observed indicating the formation of different sized or shaped particles. This is reflected in the HR-TEM image where a mixture of spherical, triangular, hexagonal and oblong shaped particles with a broad size distribution is observed (Fig. S2). Similar observations were made during the synthesis of AuNPs using fulvic acid where a decrease in pH leads to the formation of different sized particles while at higher pH monodispersed particles are obtained.⁴¹ Since the deprotonated hydroxyl groups of apigenin are assumed to reduce Au^{3+} , and as apigenin at pH 9 is found to have only two hydroxyl ions when compared to that at pH 10 (3 hydroxyl ions) it can be inferred that the polydispersed particles produced at pH 9 might be due to the inability of apigenin at this

pH to completely reduce Au^{3+} . Thus the extent of deprotonation of apigenin is found to determine the size and shape of ap-AuNPs formed.

Uptake studies

The uptake of ap-AuNPs by A431 cells has been observed through transmission electron microscopy (TEM). The representative images of the uptake of ap-AuNPs by A431 cells after a treatment period of 48 h are presented in Fig. 3. Internalization of ap-AuNPs into the sub-cellular organelles is observed. The mode of internalization of A431 cells may be by the endocytosis pathway and the absence of aggregation of ap-AuNPs inside the cell reflects a high degree of stability. Citrate reduced AuNPs are also reported to undergo such an endocytotic fate in macrophage cells.⁴⁵ Localization of AuNPs inside mitochondria and other organelles has also been observed in HeLa and MCF-7 cells.⁴⁶

Biocompatibility and cytotoxicity studies

Biocompatibility and cytotoxicity studies have been carried out with ap-AuNPs prepared at pH 10 and molar ratio of 1:4.

Haemolysis

In vitro haemolysis assay in the presence of ap-AuNPs has been carried out. The release of haemoglobin in the presence of water (positive control) represents 100 % haemolysis. Haemolysis in the presence of 50, 100, 150 and 200 $\mu\text{g} / \text{mL}$ of ap-AuNPs are found to be less than 5 % (Table 1), indicating that the ap-AuNPs are haemocompatible.

Cell viability

Cell viability has been measured through MTT assay. Fig. 4a, illustrates that ap-AuNPs do not alter the viability of HaCat cells (normal cells) even up to a period of 72 h. At a concentration as high as 200 $\mu\text{g} / \text{mL}$, the viability is 90 % indicating that ap-AuNPs are not toxic to these normal

cells. On the other hand, the percentage viability of A431 cells has been found to decrease in a concentration and time dependent manner. When treated with 100 $\mu\text{g} / \text{mL}$ of ap-AuNPs for 24 h, the viability is $72.4 \pm 2.0 \%$, which further decreases to $60.0 \pm 4.6 \%$ after 48 h. Treatment with 200 $\mu\text{g} / \text{mL}$ of ap-AuNPs for 24 and 48 h, reduces the viability to $48.3 \pm 3.3 \%$ and $37.1 \pm 3.1 \%$ respectively and a low value of $21.4 \pm 1.7\%$ is observed after 72 h treatment (Fig. 4b). The IC_{50} values obtained are 180 ± 2.3 , 130.3 ± 4.5 and $95.4 \pm 6.1 \mu\text{g} / \text{mL}$ of ap-AuNPs at 24, 48 and 72 h respectively. When A431 cells are treated with different concentrations of ct-AuNPs (50, 100 and 150 $\mu\text{g} / \text{mL}$), the viability is not altered up to 24 h. Only after 72 h, the viability decreases to $56.5 \pm 3.1\%$ on treatment with 200 $\mu\text{g} / \text{mL}$ (Fig. 4c). Comparison of the difference in the viability observed when A431 cells are treated with a similar concentration (200 $\mu\text{g} / \text{mL}$) of ap-AuNPs and ct-AuNPs indicate the enhanced cytotoxic effect of ap-AuNPs over ct-AuNPs towards A431 cells. Further, the ap-AuNPs are non-toxic to RBCs and HaCat cells at similar concentrations indicating that the action of ap-AuNPs is more specific to these cancer cells. AuNPs reduced using plant extracts such as banana stem and guava leaf are also found to be non-toxic towards normal cells, while showing anti-carcinogenicity.^{17, 47}

In order to find out whether the toxicity caused by ap-AuNPs is due to the reductant apigenin, viability assay was conducted with free apigenin at concentrations corresponding to that present on ap-AuNPs. The results show that there is no significant decrease in viability on treatment with 20 $\mu\text{g} / \text{mL}$ of free apigenin up to 72 h (Fig. 4d). A significant decrease is observed with 40 $\mu\text{g} / \text{mL}$ of free apigenin after 48 and 72 h and the viability percentages are found to be $71.0 \pm 3.5 \%$ and $65.5 \pm 2.1 \%$ respectively. It is to be noted that in the presence of 50 $\mu\text{g} / \text{mL}$ of ap-AuNPs (which contains only 10 $\mu\text{g} / \text{mL}$ of bound apigenin), similar viability values are obtained,

indicating that almost a four-fold increase in capacity to kill the cancer cells is realized by the ap-AuNPs conjugation.

The effect of ap-AuNPs on SiHa cells has also been studied. The results show a concentration and time dependent decrease in viability. On treatment with 200 $\mu\text{g} / \text{mL}$ of ap-AuNPs for 24 h, the viability is found to be $52.7 \pm 2.6 \%$, which further decreases to $44.2 \pm 3.1 \%$ and $31.8 \pm 1.1 \%$ after 48 h and 72 h respectively (Fig. S5a). Gallic acid conjugated gold nanoparticles ($150\mu\text{M}$) are reported to induce cell death in SiHa cells.⁴⁸ The viability results are comparable to that of A431 cells indicating that the ap-AuNPs exhibit comparable cytotoxicity towards these two types of epidermoid squamous carcinoma cell lines.

Microscopy Analysis

EtBr/AO and DAPI staining

The EtBr/AO staining of HaCat and A431 cells treated with different concentrations (50, 100, 150 and 200 $\mu\text{g} / \text{mL}$) of ap-AuNPs for 48 h has been carried out. Fig. 5a shows that the control and treated HaCat cells possess similar morphology and fluoresce green, which indicates that they are viable. No significant difference is observed even in the presence of a higher concentration of ap-AuNPs (200 $\mu\text{g} / \text{mL}$). But at the same time, A431 cells treated at a concentration of 50 $\mu\text{g} / \text{mL}$ of ap-AuNPs show the presence of a few dead cells (red fluorescence). The initial stage of membrane damage and reddish-orange colour stained cells are observed in the presence of 100 $\mu\text{g} / \text{mL}$ of ap-AuNPs. The loss of membrane integrity with most of the cells fluorescing red post-treatment at concentrations of 150 and 200 $\mu\text{g} / \text{mL}$ of ap-AuNPs has also been observed. Under these conditions, some cells are also found to detach from the plate (Fig. 5b).

The nuclear damage is analysed through DAPI staining. DAPI is a fluorescent chromophore, which binds to double stranded DNA. Fig. 5c shows control cells with uniform round nuclei indicating that they are viable. When 200 $\mu\text{g} / \text{mL}$ of ap-AuNPs are present, cells show crescent shaped nuclei and chromatin condensation with membrane damage, which is characteristic of apoptosis. Thus, these results suggest that the cell death brought about by ap-AuNPs may be through apoptosis.

The ap-AuNPs induced cell death on SiHa cells has also been analysed through EtBr/AO staining. Fig. S5b. shows the membrane damage and reddish-orange stained cells in the presence of 100 $\mu\text{g} / \text{mL}$ of ap-AuNPs. When treated with 200 $\mu\text{g} / \text{mL}$ of ap-AuNPs, a few cells are reddish-orange in color indicating late apoptotic phase and comparatively more number of cells are with red nuclei indicating necrosis.

DNA Fragmentation

We have further analyzed the fragmentation characteristics of DNA in the treated cells using 1% agarose gel electrophoresis. The electrophoresis pattern obtained on treatment with all concentrations of ap-AuNPs for 48 h show a ladder-like pattern indicating the presence of fragmented DNA (Fig. 6). The ladder-like pattern of DNA fragmentation confirms the occurrence of apoptosis. DNA fragmentation has been observed in MCF-7 cells on treatment with gold nanoparticles.⁴⁹

Flowcytometry analysis

Phosphatidylserine (PS) is present on the cytoplasmic surface of the cell membrane in viable cells. When the cells undergo apoptosis, PS is translocated from the inner to the outer leaflet of the plasma membrane. Annexin V is a 35-36 kDa Ca^{2+} dependent phospholipid-binding protein that has high affinity for PS and hence translocation of PS can be analysed using fluorescein

isothiocyanate (FITC) conjugated to annexin V through flow cytometry.⁵⁰ Dual staining of treated cells with annexin V-FITC and PI analysed through flow cytometry is shown in Fig.7a. Representative dot plot in the lower left quadrant denotes viable cells while the lower right and upper right quadrant populations represent early and late apoptotic cells respectively. Upper left quadrant population of cells stained only with PI denotes necrotic cells. Thus the ap-AuNPs induced cell death of A431 cells in a concentration and time dependent manner is clearly observed. The percentage of viable cells which is found to be $75.4 \pm 3.2 \%$ and $64.3 \pm 1.3 \%$ on treatment with 150 and 200 $\mu\text{g} / \text{mL}$ respectively for 24 h, decreases to $47.7 \pm 2.2 \%$ and $34.9 \pm 2.1 \%$ after 48 h. Corresponding increase in early apoptotic cell population as $12.5 \pm 1.5 \%$ and $21.1 \pm 1.6 \%$ respectively is observed after 24 h which further increases to $29.6 \pm 3.8 \%$ and $42.5 \pm 2.8 \%$ after 48 h of treatment. These results confirm that the cells undergo apoptosis on treatment with ap-AuNPs. Recently, it has been shown that *Cajanus cajan* reduced AuNPs induce early apoptosis of Hep - G2 cells which has been identified through annexin V FITC analysis.⁵¹

Cell cycle comprises four different phases (G1 phase, S phase, G2 phase and Mitosis) and two checkpoints (G0/G1 and G2/M checkpoints) which ensures that DNA damage is not transmitted to daughter cells.^{52,53} Cells treated with ap-AuNPs show gradual decrease in G0/G1 phase and corresponding increases in cell population in S - phase and Sub - G1 fraction after 24 h (Fig. 7b). An increasing S - phase population from $18.1 \pm 1.5 \%$ (control) to $27.3 \pm 0.7 \%$ (150 $\mu\text{g} / \text{mL}$ of ap-AuNPs) and 29.3 ± 2.5 (200 $\mu\text{g} / \text{mL}$ of ap-AuNPs) indicates cell cycle arrest in S-phase. The percentage of Sub - G1 population is $1.8 \pm 0.6 \%$ in control, whereas after treatment with 50, 100 and 150 $\mu\text{g} / \text{mL}$ of ap-AuNPs for 24 h, the values are $5.6 \pm 1.5 \%$, $10.1 \pm 0.4 \%$ and 13.8 ± 2.7

% respectively. For the same time period, the value further increases to 21.7 ± 3.2 % in the presence of $200 \mu\text{g} / \text{mL}$ of ap-AuNPs. The Sub - G1 population is as high as 31.1 ± 4.3 % after 48 h of treatment with $200 \mu\text{g} / \text{mL}$ of ap-AuNPs, with a concomitant decrease in G0/G1 (29.8 ± 2.3 %) and G2/M (12.6 ± 1.6 %) phases. The increase in Sub - G1 population with increase in ap-AuNPs concentration and treatment period also indicates the apoptotic mode of cell death. Thus, the characteristic morphological features of apoptosis observed through EtBr / AO and DAPI staining are confirmed through DNA fragmentation and flow-cytometric analysis. AuNPs have been reported to induce apoptosis of several cancer cells via S phase and Sub - G1 arrest.^{50,53,54}

Anti-angiogenic potential exerted by ap-AuNPs (CAM assay)

To test if ap-AuNPs possess anti-angiogenic activity, *in vivo* chick embryo chorioallantoic membrane (CAM) assay has been performed. CAMs were treated with different concentrations of ap-AuNPs for 48 h. The ap-AuNPs at a concentration of $200 \mu\text{g} / \text{mL}$ inhibits the formation of new blood vessels and sub branches when compared to that of control and VEGF treated chick embryos (Fig. 8). Though the ability of pure apigenin ($20 \mu\text{M}$) to inhibit angiogenesis in prostate cancer cells through HIF and VEGF expression has been demonstrated³⁰ that apigenin capped AuNPs (ap-AuNPs) can also limit the growth of new blood capillaries is demonstrated in this study. The results on the ability of ap-AuNPs to inhibit the development of blood vessels indicate their anti-angiogenic property implying their value as agents for skin cancer treatment.

Materials and Methods

Hydrogen tetrachloroaurate ($\text{HAuCl}_4 \cdot 3\text{H}_2\text{O}$, >99.9%), apigenin, Dulbecco's Modified Eagle's Medium (DMEM), phosphate buffered saline (PBS), sodium bicarbonate, streptomycin, gentamicin, penicillin, amphotericin B, trypsin - EDTA, ethidium bromide (EtBr), acridine

orange (AO), 3-(4, 5-Dimethylthiazol-2-yl)-2, 5-diphenyltetrazolium bromide (MTT), 4'-6-diamidino-2-phenylindole (DAPI), agarose, propidium iodide (PI), DNase free RNase, proteinase K, 4-(2-hydroxyethyl)-1-piperazineethane sulfonic acid (HEPES), ethylenediaminetetracetic acid (EDTA) and dimethylsulphoxide (DMSO) were purchased from Sigma Aldrich (USA). Fetal Bovine Serum (FBS) was purchased from GIBCO (USA). Ammonium acetate, Nonidet P- 40, potassium carbonate (K_2CO_3), potassium bromide (KBr), tris hydrochloride and formaldehyde were obtained from Merck (USA). Annexin - V- FITC apoptosis kit was obtained from BD Bioscience, USA. Dodecyl succinic acid (DDSA), epon 812 resin, glutaraldehyde, lead citrate, nadic methyl anhydride (NMA), sodium cacodylate buffer and uranyl acetate were bought from EM Sciences, USA. MilliQ water (conductivity of $18 \text{ m}\Omega \text{ cm}^{-1}$) was autoclaved and filter-sterilised using $0.22 \text{ }\mu\text{m}$ filters. Cells (A431, HaCat and SiHa) were obtained from the National Centre for Cell Science, Pune, India.

Synthesis of apigenin conjugated gold Nanoparticles (ap-AuNPs)

A stock solution of 10 mM apigenin was prepared by dissolving in 100 % DMSO. Aqueous stock solution of $H AuCl_4$ (10 mM) and K_2CO_3 (150 mM) were prepared in filtered MilliQ water. The pH of the apigenin solution (0.3 mM) was adjusted to 10 using K_2CO_3 . Then, 1.2 mM of $H AuCl_4$ was added drop wise while mixing the solution of apigenin at RT. The reduction of Au^{3+} to Au^0 was monitored spectrophotometrically (280-900 nm) using a multimode plate reader (Tecan Infinite M 200). Reduction was also assessed using different concentrations of $H AuCl_4$ (0.3 to 1.6 mM) and at different pH values (8-11). The resultant ap-AuNPs solution was allowed to age at RT for 4 days and centrifuged at 15000 X g for 10 min at a temperature of 15° C . The pellet was resuspended with MilliQ water and washed thrice to eliminate unreacted apigenin and $H AuCl_4$. Finally, the pellet was resuspended in MilliQ water and then used for further

characterisation. Citrate reduced gold nanoparticles (ct-AuNPs) were also prepared by reacting sodium citrate and HAuCl_4 in the ratio of 1: 6.8.⁵⁵ This has been used as a control for comparing the cytotoxicity of ap-AuNPs.

Characterisation of ap-AuNPs

Electron microscopic study

For this, the ap-AuNPs were loaded onto carbon coated copper grids and allowed to air dry. The size and shape of the ap-AuNPs were viewed using HR-TEM (FEI, TECNAI T 20 G²) operated at 300 kV.

X-Ray diffraction analysis (XRD)

The lyophilized powder of ap-AuNPs were subjected to X-ray diffraction analysis (Seifert JSO-Debye flex 2002) at an operating voltage of 40 kV and a current of 30 mA with $\text{CuK}\alpha 1$ radiation (wavelength = 1.54056 \AA). The scan range was set between 20 and 80°.

Dynamic Light Scattering (DLS) and Zeta potential

The zeta potential and hydrodynamic diameter (size) of ap-AuNPs were analysed using Malvern Zetasizer version 6.2.

Fourier transform infrared spectroscopy (FT-IR)

KBr pellets of apigenin and ap-AuNPs were prepared and FT-IR spectra were recorded in a Nicolet spectrometer in transmission mode from 500 to 3500 cm^{-1} .

Thermogravimetric analysis (TGA)

TGA of the lyophilised powder of ap-AuNPs was performed with a TGA analyser (TGA Q 50-TA instruments). The ramp was set at 20 °C/min range from 30 °C to 800 °C under nitrogen atmosphere.

Atomic Absorption Spectrophotometry (AAS)

The concentration of Au in the ap-AuNPs was determined by atomic absorption spectrophotometry (AAS) using Analytik Jena (AAS novAA 350 BU) instrument.

Biocompatibility of ap-AuNPs: Haemolysis assay

Haemocompatibility studies were performed after getting approval from the Institutional Review Board (IRB) of Central Leather Research Institute (CLRI), Chennai, India. Blood was collected from healthy donors in a heparinised tube and red blood cells (RBCs) were separated by centrifugation. The isolated RBCs were washed four times with Dulbecco's phosphate buffered saline (PBS) at 400 X g for 5 min, and then diluted 10 times with PBS. To 0.2 mL of RBCs, 0.8 mL of different concentrations of ap-AuNPs in PBS were added and incubated for 4 h at 37°C. The cells were then vortexed and centrifuged at 400 X g for 10 min. The absorbance of haemoglobin was measured at 577 nm in 200 µl of the supernatant with reference wavelength at 655 nm in a multimode plate reader (Tecan Infinite M 200). Water and PBS served as positive and negative controls respectively. The percentage of haemolysis was calculated using the formula as below

$$\% \text{Haemolysis} = \frac{\text{absorbance of sample} - \text{absorbance of negative control}}{\text{absorbance of positive control} - \text{absorbance of negative control}} \times 100$$

Cell Culture

Cells were grown in DMEM medium containing 10 % FBS, 100 µg / ml streptomycin, 100 µg / ml gentamycin, 100 U / ml penicillin and 2.5 µg / ml amphotericin B. Cells were trypsinized at 70 - 80 % confluency using 0.25 % trypsin - EDTA and seeded for the experiments. The cells were allowed to attach overnight and then treated with ap-AuNPs while untreated cells served as control. The cells were maintained at 37 °C with 5% CO₂ in a CO₂ incubator (Binder, Germany).

Uptake studies

For TEM analysis, 1×10^6 cells were grown in a T25 flask and treated with $100 \mu\text{g}/\text{mL}$ of ap-AuNPs for 48 h. After incubation, the cells were washed thrice with PBS and trypsinized. The cells were then fixed with 2.5% of glutaraldehyde prepared in 0.1 M sodium cacodylate buffer (pH 7.4) for 4 h. The pellet was then centrifuged and washed with the same buffer thrice for 10 min each. They were then post fixed in 0.1% osmium tetroxide prepared in the same buffer for 2 h at 8°C and further washed as above. The cells were pelleted through centrifugation after each step and further dehydrated through a graded series of acetone 30%, 50%, 70%, 80%, and 90% for 10 min. It was then treated with 100% acetone twice for 10 min, each time followed by propylene oxide treatment for 10 min. The pellet was then infiltrated with resin mixture consisting of Epon 812 resin, DDSA and NMA starting with 25%, 50% and 75% for 2 h and 100% overnight. It was then embedded in the same resin mixture with catalyst (DMP 30) in “easymoulds” at 60°C for 48 h. Ultra thin sections from the resin block were cut and stained with saturated solutions of uranyl acetate and lead citrate. After air drying, the sections were visualized in Jeol JEM 1400 transmission electron microscope at 80 kV and micrographs acquired using Olympus Keen view CCD camera.

MTT viability assay

The viability of HaCat, A431 and SiHa cells on exposure to ap-AuNPs were determined by MTT assay. Cells (1×10^4) were treated with various concentrations of ap-AuNPs for 0 - 72 h. A431 cells were also treated with apigenin, ct-AuNPs and compared with that of ap-AuNPs. They were then washed with sterile PBS and incubated with MTT ($0.5 \text{ mg}/\text{mL}$) solution for 4 h at 37°C . The formazan product formed was dissolved in $200 \mu\text{l}$ of DMSO and the absorbance was measured at 570 nm using a reference wavelength of 630 nm in a multimode plate reader (Tecan Infinite M 200). Viability test was also conducted on cells treated with 10, 20, 30 and $40 \mu\text{g}/\text{mL}$

of free apigenin. Experiments were conducted in triplicate and the percentage of viable cells was calculated with respect to control.

Microscopy studies

Ethidium Bromide / Acridine Orange staining (EtBr /AO)

Cells were grown on cover slips and treated with different concentrations of ap-AuNPs. After the incubation period, the cells were washed and stained with 10 μg each of EtBr and AO in PBS. They were immediately viewed using a confocal laser scanning microscope (450 – 490 nm) (Nikon Eclipse E600, Japan) and images were acquired using EZ-C1 software.

DAPI Staining

Treated cells were washed with PBS and fixed with 4% formaldehyde in PBS for 30 min at RT. After washing with PBS, the cells were stained with DAPI (1 μg / mL) dye for 10 min in the dark. They were immediately viewed using a confocal laser scanning microscope (350 – 470 nm) (Leica, TCS SP 2-X1, Germany) and images were acquired using EZ-C1 software.

DNA Fragmentation

A431 cells (3×10^6) seeded in 6 well plates and grown in DMEM medium were exposed to different concentrations of ap-AuNPs for 48 h. DNA was isolated according to the method described by Hermann et al. (1994). Cells were centrifuged at 400 X g for 10 min, washed with PBS and were lysed using DNA lysis buffer (50 mM Tris-HCl (pH 7.5), 20 mM EDTA and 1% NP-40) on ice. The cell lysates were then incubated with 5 mg / mL of RNase and 1% SDS for 2 h at 56 °C and then at 37 °C for 2 h with 2.5 mg / mL of proteinase K. DNA was precipitated with 0.5 volumes of 10 mM ammonium acetate and 2.5 volumes of ice-cold ethanol (70%) at -80 °C overnight. The DNA was collected by centrifugation at 13000 X g for 20 min and dissolved

in Tris - EDTA buffer. The DNA samples were subjected to electrophoresis on 1% agarose gel and the image was documented using Gel Documentation system (Bio - Rad, USA).

Flow-cytometry Analysis

1×10^6 cells were grown in tissue culture (6 wells) plates and treated with different concentrations of ap-AuNPs for 24 and 48 h. Cells were pelleted, resuspended in the 1X binding buffer and stained with Annexin V- FITC and PI according to the manufacturer's instructions. After 20 min of incubation in the dark, the fluorescence intensities were measured with the FL1 channel (FITC - 518 nm) and FL2 channel (PI - 620 nm) using a flow cytometer (BD FACS Calibur, USA).

For cell cycle analysis, treated cells were trypsinized, fixed with 70 % ethanol and stored at -20°C overnight. They were then suspended in 0.5 mL of sterile PBS containing $50 \mu\text{g} / \text{mL}$ of DNase free RNase and $50 \mu\text{g} / \text{mL}$ of PI at RT in the dark for 20 min. From the fluorescence measured at 488 nm using flow cytometer, the cells present in the various phases were analysed using Cell Quest Pro software.

Chorioallantoic membrane (CAM) assay

The effect of ap-AuNPs on angiogenesis was evaluated using chorioallantoic membrane (CAM) assay. For this, fertilized chick eggs (seven days old) were purchased from a local hatchery and incubated at 37°C and 60 % humidity level. On the seventh day of incubation, a window was opened on the egg shell over the air sac region. Sterilized filter paper discs saturated with PBS, VEGF (positive control), Doxorubicin (negative control) or different concentrations of ap-AuNPs were placed on the CAM and incubated as mentioned above. The formation of blood vessels was observed after 48 h of treatment period. The assay was conducted in triplicates for each concentration.

Statistical analysis

All data were expressed as mean \pm S.D of three independent experiments and statistical evaluations were performed with two - way ANOVA followed by Bonferroni post-tests using GraphPad Prism5 (GraphPad Prism software Inc., USA). Data were considered as statistically significant with $p < 0.05$.

Conclusion

Our study on the synthesis of ap-AuNPs using apigenin has revealed that Au^{3+} can be reduced by apigenin at a pH of 10 and at RT forming highly stable and spherical ap-AuNPs. These ap-AuNPs are biocompatible towards normal epidermoid cells (HaCat) while inducing apoptosis of A431 and SiHa cells at the concentrations used here. The ap-AuNPs also exhibit good anti-angiogenic property. Hence, ap-AuNPs can be considered as a promising candidate for use in skin cancer treatment.

The authors have no conflict of interest.

Acknowledgement

The authors thank the Director, CLRI, Chennai, India for providing the necessary facilities and support. The work was carried out with financial assistance through the Council of Scientific and Industrial Research, India, XII five year plan project (Nano SHE -BSC 0112). The authors thank the staff of TEM facilities of the National Centre for Nanoscience and Nanotechnology, University of Madras and the Cancer Institute, Chennai.

REFERENCES

- 1.R.S. Laishram, A. Banerjee, P. Punyabati and L.D.C. Sharma, *J Pak Assoc Derma.*, 2010, 20, 128 - 132.

- 2.M.R. Karagas, T.A. Stukel, J.S. Morris, T.D. Tosteson, J.E. Weiss, S.K. Spencer and E.R. Greenberg, *Am J Epidemiol.*, 2001, 153, 559 - 565.
- 3.V. Peharda, F. Gruber, M. Kastelan, L.P. Massari, M. Saftic, L. Cabrijan and G. Zamolo, *Coll Antropol.*, 2007, 31, 87 - 90.
- 4.F. Gruber, V. Peharda, M. Kastelan and I. Brajac, *Acta Dermatovenerol Croat.*, 2007, 15, 191 - 198.
- 5.A. Llevot and D. Astruc, *Chem Soc Rev.*, 2012, 41, 242 - 257.
- 6.R.M. Navalakhe and T.D. Nandedkar, *Ind J Exp Biol.*, 2007, 45, 160 - 165.
- 7.P.M. Tiwari, K. Vig, V.A. Dennis and S.R. Singh, *Nanomaterials*, 2011, 1, 31 - 63.
- 8.E.E. Bedford, J. Spadavecchia, C.M. Pradier and F.X. Gu, *Macromol Biosci.*, 2012, 12, 724 - 739.
- 9.X.Q. Zhao, T.X. Wang, W. Liu, C.D. Wang, D. Wang, T. Shang, L. Shen and L. Ren, *J Mater Chem.*, 2011, 21, 7240 - 7247.
- 10.C. Pache, N.L. Bocchio, A. Bouwens, M. Villiger, C. Berclaz, J. Goulley, M.I. Gibson, C. Santschi and T. Lasser, *Optics express.*, 2012, 20, 21385 - 21399.
- 11.S. Vijayakumar and S. Ganesan, *J Nanomater.*, 2012, 1 - 9.
- 12.S. Sasidharan, A. Jayasree, S. Fazal, M. Koyakutty, S.V. Nair and D. Menon, *Biomater Sci.*, 2013, 1, 294 - 305.
- 13.C. Freese, C. Uboldi, M.I. Gibson, R.E. Unger, B.B. Weksler, I.A. Romero, P.O. Couraud and C.J. Kirkpatrick, *Part Fibre Toxicol.*, 2012, 9, 1 - 11.
- 14.D. Raghunandan, S. Basavaraja, B. Mahesh, S. Balaji, S.Y. Manjunath and A. Venkataraman, *Nanobiotechnology*, 2009, 5, 34 - 41.
- 15.K.B. Narayanan and N. Sathivel, *Mater Lett.*, 2008, 62, 4588 - 4590.

- 16.S.K. Nune, N. Chanda, R. Shukla, K. Katti, R.R. Kulkarni, S. Thilakavathy, S. Mekapothula, R. Kannan and K.V. Katti, *J Mater Chem.*, 2009, 19, 2912 - 2920.
- 17 R.K. Mohanty, S. Thennarasu and A.B. Mandal, *Colloids Surf B Biointerfaces.*, 2014, 114, 138 - 143.
- 18.S.A. Aromal and D. Philip, *Physica E.*, 2012, 44, 1692 - 1696.
- 19.A. Vijayalakshmi, P.R. Kumar, S.S. Priyadarsini and C. Meenaxshi, *J Chem.*, 2013, 1 - 9.
- 20.P. Batra and A.K. Sharma, *Biotech*, 2013, 3, 439 - 459.
- 21.J. Kasthuri, S. Veerapandian and N. Rajendiran, *Colloids Surf B Biointerfaces.*, 2009, 68, 55 - 60.
- 22.Q. Guo, Q.Guo, J. Yuan and J. Zeng, *colloids surf A Physicochem eng asp.*, 2014, 441, 127 - 132.
- 23.D.K. Das, A. Chakraborty, S. Bhattacharjee and S. Dey, *J Exp Nanoscience*, 2013, 8, 649 - 655.
- 24.B.K. Jena, B.K. Mishra and S. Bohidar, *J Phys Chem C.*, 2009, 113, 14753 - 14758.
- 25.J. Cao, W. Chen, Y. Zhang, Y. Zhang and X. Zhao, *Food Sci Technol Res.*, 2010, 16, 395 - 402.
- 26.S. Balasubramanian and R.L. Eckert, *Toxicol Appl Pharmacol.*, 2007, 224, 214 - 219.
- 27.H. Wei, L. Tye, E. Bresnick and D.F. Birt, *Cancer Res.*, 1990, 50, 499 - 502.
- 28.S. Shukla and S. Gupta, *Free Radical Biol Med.*, 2008, 44, 1833 - 1845.
- 29.J. Fang, C. Xia, Z. Cao, J.Z. Zheng, E. Reed and B.H. Jiang, *FASEB J.*, 2005, 19, 343 - 353.
- 30.J. Fang, Q. Zhou, L.Z. Liu, C. Xia, X. Hu, X. Shi and B.H. Jiang, *Carcinogenesis.*, 2007, 28, 858 - 864.

- 31.H. Shao, K. Jing, E. Mahmoud, H. Huang, X. Fang and C. Yu, *Mol Cancer Ther.*, 2013, 12, 2640 - 2650.
- 32.Y. Zhu, Y. Mao, H. Chen, Y. Lin, Z. Hu, J. Wu, X. Xu, X. Xu, J. Qin and L. Xie, *Cancer Cell Int.*, 2013, 13, 1 - 7.
- 33.X. Cao, B. Liu, W. Cao, W. Zhang, F. Zhang, H. Zhao, R. Meng, L. Zhang, R. Niu, X. Hao and B. Zhang, *Chin J Cancer Res.*, 2013, 25, 212 - 222.
- 34.S. Das, J. Das, A. Samadder, N. Boujedaini and A.R.K. Bukhsh, *Exp Biol Med.*, 2012, 237, 1433 - 1448.
- 35.S. Das, J. Das, A. Samadder, A. Paul and A.R.K. Bukhsh, *Food Chem Toxicol.*, 2013, 62, 670 - 680.
- 36.S. Kondath, S.R. Bhuvanaree, A. Rajaram and R. Rajaram, *Chem Biol Interact.*, 2014, 224, 78 - 88.
- 37.B. Li, D.H. Robinson and D.F. Birt, *J. Pharma Sci.*, 1997, 86, 721 - 725.
- 38.K. Sindhu, A. Rajaram, K.J. Sreeram and R. Rajaram, *RSC Adv.*, 2014, 4, 1808 - 1818.
- 39.B.K. Pong, H.I. Elim, J.X. Chong, W. Ji, B.L. Trout and J.Y. Lee, *J Phys Chem C.*, 2007, 111, 6281 - 6287.
- 40.A. Rai, A. Singh, A. Ahmad and M. Sastry, *Langmuir*, 2006, 22, 736 - 741.
- 41.D.S.D. Santos, J. Ramon, A.A. Puebla, O.N. Oliveira and R.F. Aroca, *J Mater Chem.*, 2005, 15, 3045 - 3049.
- 42.G. Mariappan, N. Sundaraganesan, S. Manoharan, *Spectrochim Acta A Mol Biomol Spectros.*, 2012, 95, 86 - 99.
- 43.B.P. Pawłęga, L.E. Misiak, B. Zarzyka, R.P.A. Gawron and W.I. Gruszecki, *Biochim Biophys Acta*, 2013, 1828, 518 - 527.

- 44.R. Pal, S. Panigrahi, D. Bhattacharyya and A.S. Chakraborti, *J Mol Struct.*, 2013, 1046, 153 - 163.
- 45.R. Shukla, V. Bansal, M. Chaudhary, A. Basu, R. R. Bhonde and M. Sastry, *Langmuir*, **2005**, *21*, 10644 - 10654.
- 46.K. Song, P. Xu, Y. Meng, F. Geng, J. Li, Z. Li, J. Xing, J. Chen and B. Kong, *Int. J. Oncol.*, 2013, *42*, 597 - 608.
- 47.P. Arunkumar, H. Vedagiri and K. Premkumar, *J Nanopart Res.*, 2013, *15*, 1 - 8.
- 48.J. Daduang, A. Palasap, S. Daduang, P. Boonsiri, P. Suwannalert and T. Limpai boon, *Asian Pac J Cancer Prev.*,2015, *16*, 169 - 174
49. S. Varun and S. Sellappa, *Int J Pharm Pharm Sci.*, 2014, *6*, 528 - 531
- 50.G. Zhang, V. Gurtu, S.R. Kain and G. Yan, *BioTechniques.*, 1997, *23*, 525 - 531.
- 51.A.Thirunavukkarasu, P. Durai, G. Ravi, G. Kasivelu, M. Ramar, A. Chinnasamy and S. Ganesan, *Colloids Surf B Biointerfaces.*, 2014, *123*, 549-311.
- 52.P. Pozarowski and Z. Darzynkiewicz, *Methods Mol Biol.*, 2004, *281*, 301 - 311.
- 53.K.T. Butterworth, J.A. Coulter, S. Jain, J. Forker, S.J. McMahon, G. Schettino, K.M. Prise, F.J. Currell and D.G. Hirst, *Nanotechnology.*, 2010, *23*, 1 - 18.
- 54.M. Jeyaraj, R. Arun, G. Sathishkumar, D. MubarakAli, M. Rajesh, G. Sivanandhan, G. Kapildev, M. Manickavasagam, N. Thajuddin and A. Ganapathi, *Mater Res Bull.*, 2014, *52*, 15 - 24.
- 55.I. Ojea-Jimenez, N.G. Bastus and V. Puentes, *J. Phys. Chem. C.*, 2011, *115*, 15752 – 15757.

Figure Captions

Fig. 1 UV –Visible spectra of the ap-AuNPs formed at different conditions of synthesis (a) ap-AuNPs formed at different pHs of apigenin (0.3 mM of apigenin and 1.2 mM of HAuCl₄ is used for the synthesis); inset picture shows burgundy red color of ap-AuNPs formed at pH 10 (b) ap-AuNPs formed at different molar ratios of apigenin to HAuCl₄ reacted at pH 10 (Concentration of apigenin has been kept constant at 0.3 mM and the concentration of HAuCl₄ ranges from 0.3 to 1.5 mM) and (c) Kinetics of ap-AuNPs formation

Fig. 2 Characterization of ap-AuNPs formed at pH 10 (a) Low magnification HR-TEM image with inset showing the size distribution of ap-AuNPs (b) A single particle of ap-AuNPs depicting lattice fringes (c) SAED pattern depicting the lattice planes of Au in ap-AuNPs (d) X-ray diffraction pattern illustrating crystalline nature of the ap-AuNPs (e) size of ap-AuNPs measured by DLS (f) stability of ap-AuNPs measured by Zeta potential (g) FTIR spectrum of apigenin and ap-AuNPs (h) TGA showing the different phases of weight loss of the reductant apigenin on the ap-AuNPs

Fig. 3 Uptake of ap-AuNPs in A431 cells as seen by Transmission Electron Microscopy (a) internalization of ap-AuNPs (b) magnified image showing dispersed ap-AuNPs sequestered in phagolysosomes

Fig. 4 Viability assay measured using MTT. The effect of ap-AuNPs on (a) HaCat cells (b) A431 cells (c) Effect of ct-AuNPs on A431 cells and (d) Effect of free apigenin on A431 cells. The values represent mean \pm SD of three independent experiments. * $p < 0.05$, ** $p < 0.01$ and *** $p < 0.001$ vs control.

Fig. 5 Fluorescence micrographs using EtBr/AO staining of (a) HaCat cells and (b) A431 cells on treatment with ap-AuNPs. The morphological changes are indicated as early apoptotic (\longrightarrow), late apoptotic (\longrightarrow \blacklozenge) and necrotic cells (\longrightarrow \blacktriangleright) (c) Fluorescence micrographs

using DAPI staining. The morphological changes are indicated as apoptotic bodies (—▶), chromatin condensation (—●) and chromatin condensation with membrane damage (—▶).

Fig. 6 DNA fragmentation assessed using 1% of agarose gel electrophoresis. Genomic DNA extracted from A431 cells without (control) and after treatment with various concentration of ap-AuNPs for 48h.

Fig. 7 Flow cytometry analyses of A431 cells on treatment with different concentration of ap-AuNPs. (a) Annexin - V - FITC binding and PI uptake (b) Cell cycle analysis using PI fluorescence. Dot plots and histogram plots are representative of three independent experiments.

Fig. 8 The anti-angiogenic potential of ap-AuNPs analyzed using CAM assay. Arrows point to the presence of blood vessels (control and VEGF) and inhibition of existing blood vessels in ap-AuNPs treated CAM.

Supplementary figures

Fig. S1 Comparison of bandwidth values of ap-AuNPs (a) at different pH (molar ratio 1:4) (b) at different molar ratio (pH 10).

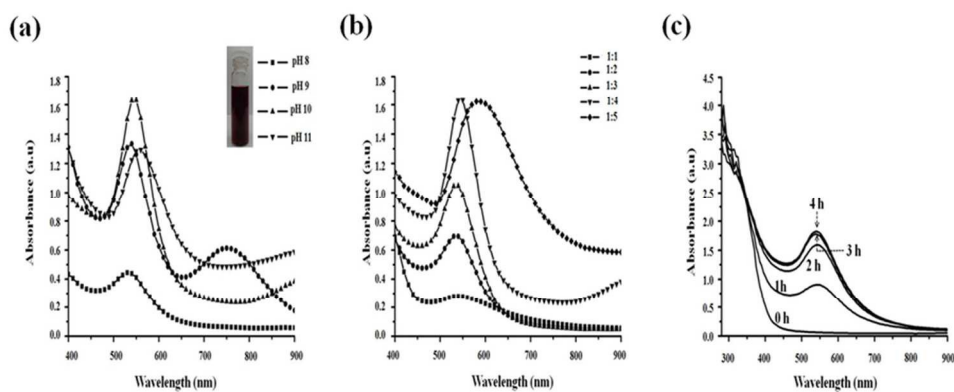
Fig. S2 Morphology of ap-AuNPs prepared at pH 9 as analysed through HR-TEM (a & b) Different shapes of ap-AuNPs and inset shows the size distribution histogram (c) The SAED pattern of Au in the ap-AuNPs.

Fig. S3 UV- visible spectra of ap-AuNPs showing stability at pH 10 after 3 months

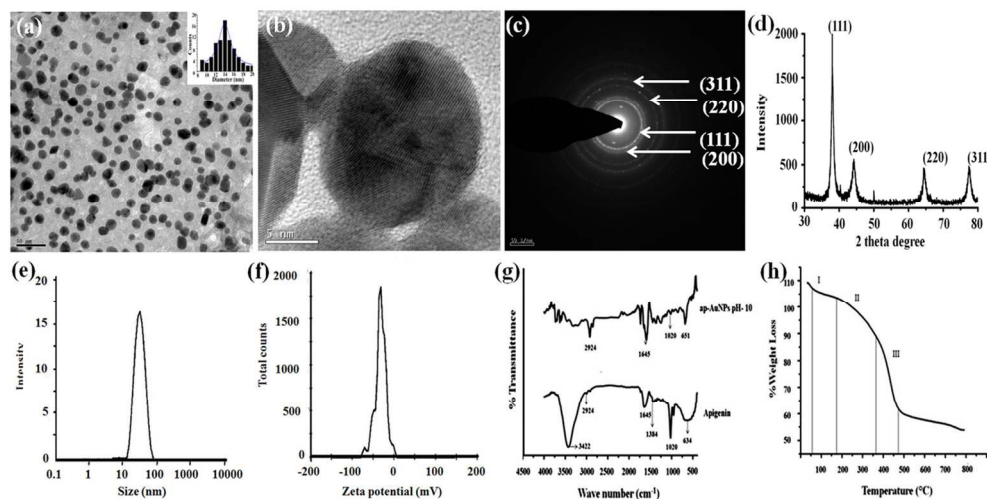
Fig. S4 FTIR spectra of apigenin and ap-AuNPs prepared using apigenin at pH 9

Fig. S5 Effect of ap-AuNPs on SiHa cells (a) Viability assay using MTT (b) Fluorescence micrographs using EtBr/AO staining of SiHa cells for 48 h. The morphological changes are indicated as early apoptotic (—▶), late apoptotic (—▶) and necrotic cells (—▶)

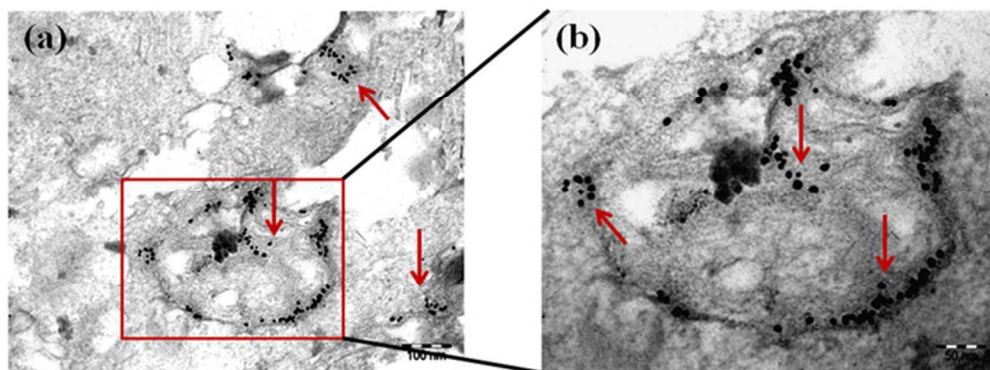
Table. 1 Showing the haemocompatibility of ap-AuNPs.



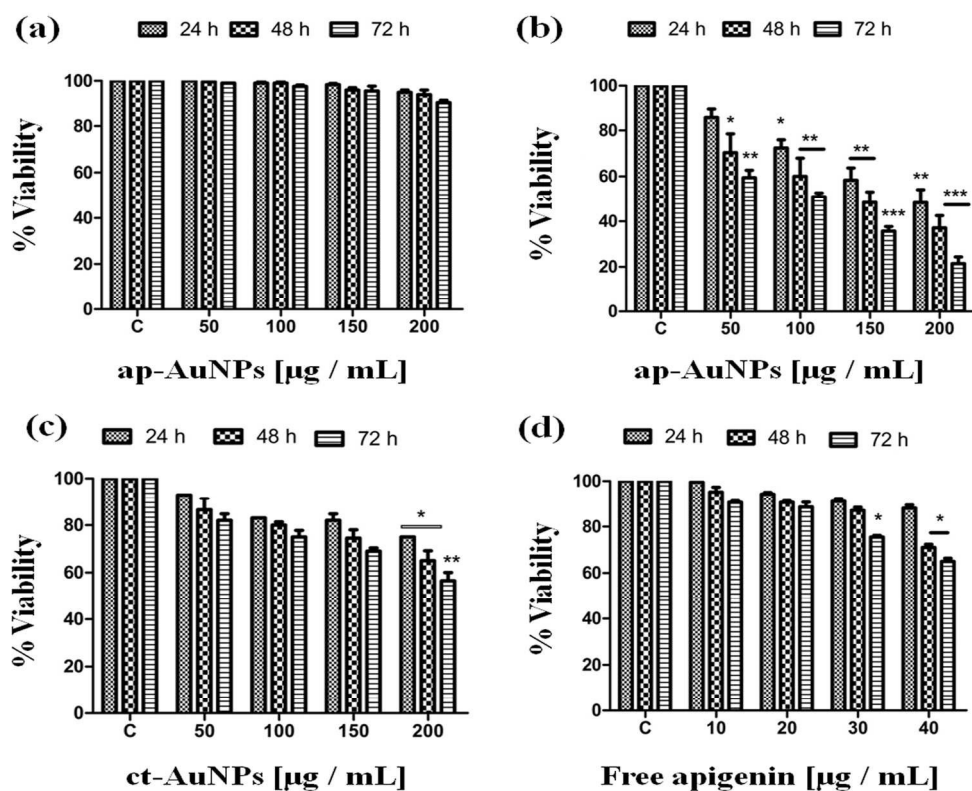
UV -Visible spectra of the ap-AuNPs formed at different conditions of synthesis (a) ap-AuNPs formed at different pHs of apigenin (0.3 mM of apigenin and 1.2 mM of HAuCl₄ is used for the synthesis); inset picture shows burgundy red color of ap-AuNPs formed at pH 10 (b) ap-AuNPs formed at different molar ratios of apigenin to HAuCl₄ reacted at pH 10 (Concentration of apigenin has been kept constant at 0.3 mM and the concentration of HAuCl₄ ranges from 0.3 to 1.5 mM) and (c) Kinetics of ap-AuNPs formation 40x16mm (600 x 600 DPI)



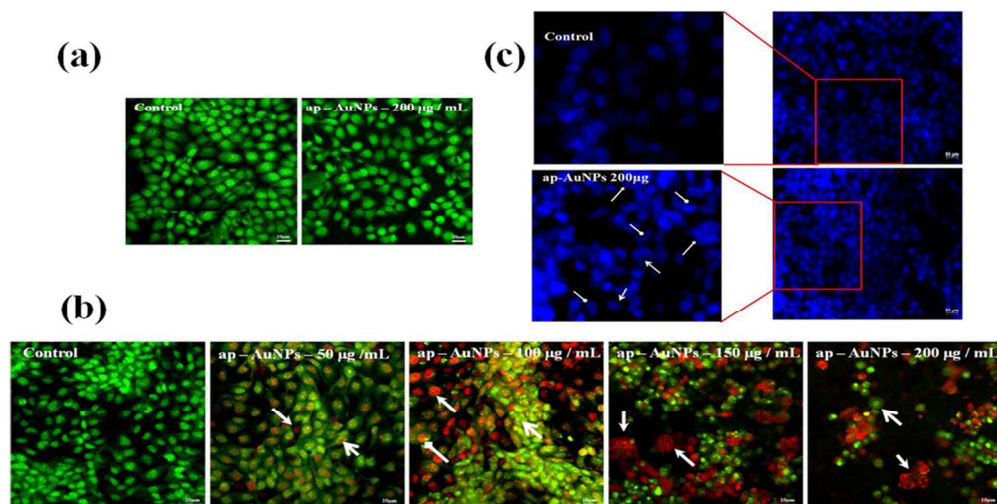
Characterization of ap-AuNPs formed at pH 10 (a) Low magnification HR-TEM image with inset showing the size distribution of ap-AuNPs (b) A single particle of ap-AuNPs depicting lattice fringes (c) SAED pattern depicting the lattice planes of Au in ap-AuNPs (d) X-ray diffraction pattern illustrating crystalline nature of the ap-AuNPs (e) size of ap-AuNPs measured by DLS (f) stability of ap-AuNPs measured by zeta potential (g) FTIR spectrum of apigenin and ap-AuNPs (h) TGA showing the different phases of weight loss of the reductant apigenin on the ap-AuNPs
59x30mm (600 x 600 DPI)



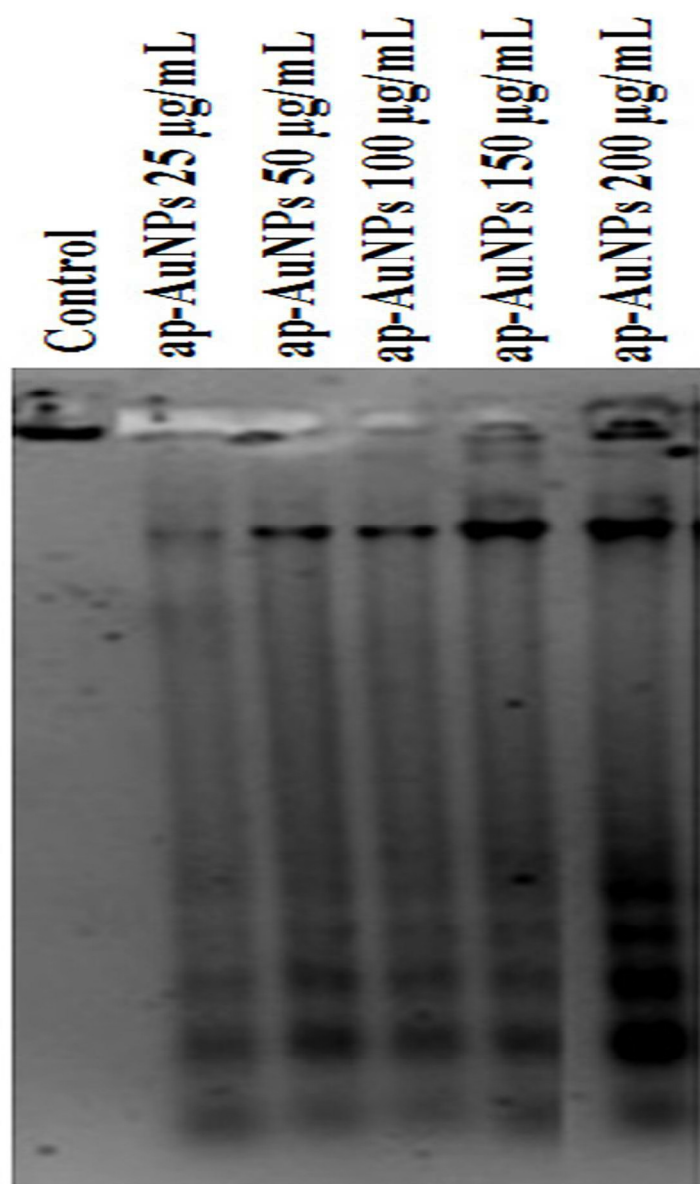
Uptake of ap-AuNPs in A431 cells as seen by Transmission Electron Microscopy (a) internalization of ap-AuNPs (b) magnified image showing dispersed ap-AuNPs sequestered in phagolysosomes
29x11mm (600 x 600 DPI)



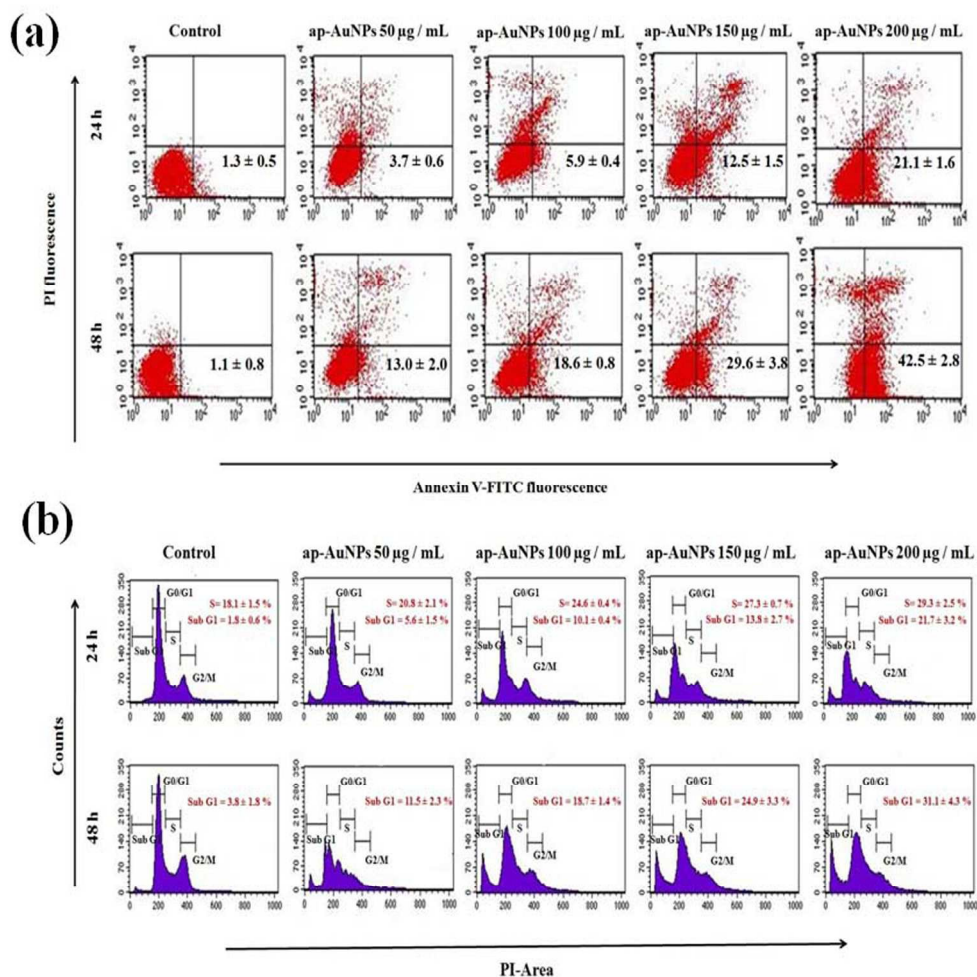
Viability assay measured using MTT. The effect of ap-AuNPs on (a) HaCat cells (b) A431 cells (c) Effect of ct-AuNPs on A431 cells and (d) Effect of free apigenin on A431 cells. The values represent mean \pm SD of three independent experiments. * $p < 0.05$, ** $p < 0.01$ and *** $p < 0.001$ vs control.
80x64mm (600 x 600 DPI)



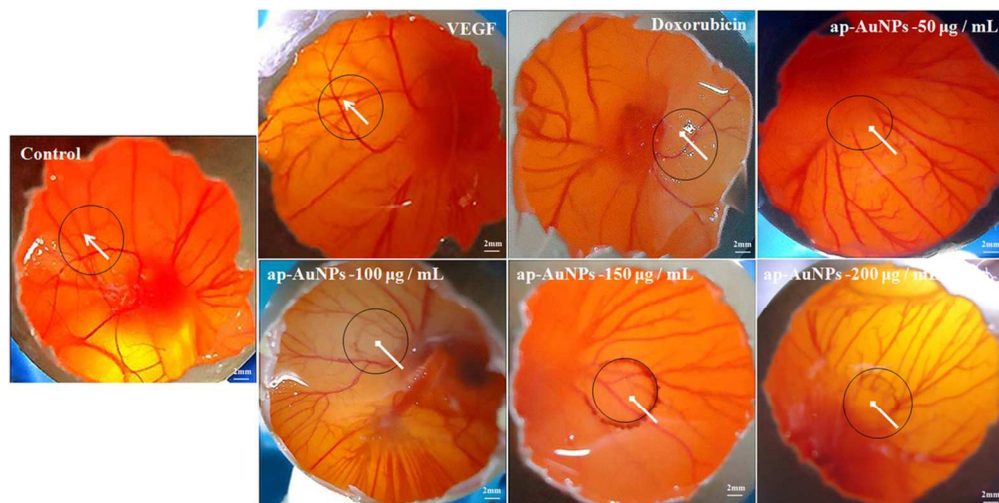
Fluorescence micrographs using EtBr/AO staining of (a) HaCat cells and (b) A431 cells on treatment with ap-AuNPs. The morphological changes are indicated as early apoptotic (), late apoptotic () and necrotic cells () (c) Fluorescence micrographs of A431 cells using DAPI staining. The morphological changes are indicated as apoptotic bodies (), chromatin condensation () and chromatin condensation with membrane damage ().
49x25mm (600 x 600 DPI)



DNA fragmentation assessed using 1% of agarose gel electrophoresis. Genomic DNA extracted from A431 cells without (control) and after treatment with various concentration of ap-AuNPs for 48h.
49x83mm (600 x 600 DPI)



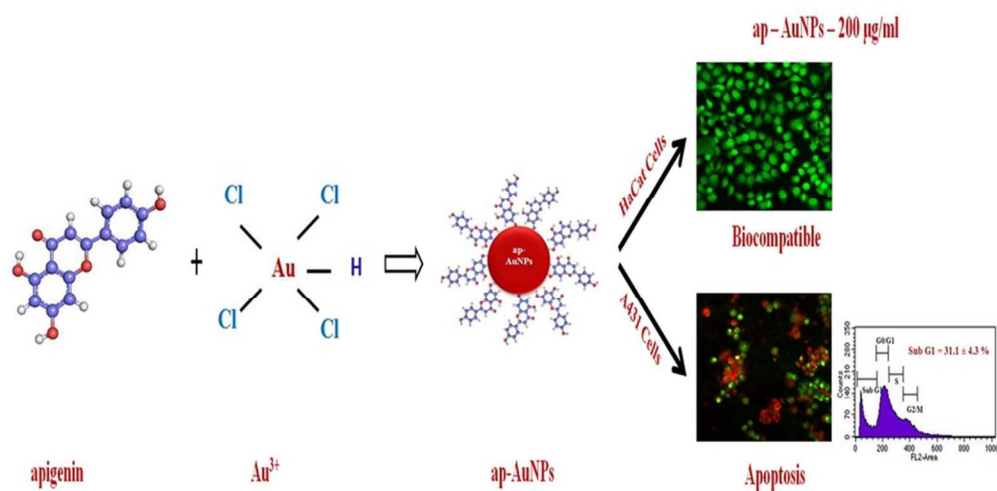
Flow cytometry analyses of A431 cells on treatment with different concentration of ap-AuNPs. (a) Annexin - V - FITC binding and PI uptake (b) Cell cycle analysis using PI fluorescence. Dot plots and histogram plots are representative of three independent experiments. 99x99mm (600 \times 600 DPI)



The anti-angiogenic potential of ap-AuNPs analyzed using CAM assay. Arrows point to the presence of blood vessels (control and VEGF) and inhibition of existing blood vessels in ap-AuNPs treated CAM.
49x25mm (600 x 600 DPI)

Table. 1 Haemocompatibility of ap-AuNPs.

Sample	% of Haemolysis
Positive control - Water	100 ± 0.0
Negative Control - PBS	1.9 ± 0.2
ap-AuNPs 50 µg/mL	1.0 ± 0.0
ap-AuNPs 100 µg/mL	1.0 ± 0.1
ap-AuNPs 150 µg/mL	1.7 ± 0.2
ap-AuNPs 200 µg/mL	2.6 ± 0.1



Apigenin reduces Au^{3+} to Au^0 to form ap-AuNPs at RT. ap-AuNPs are biocompatible towards HaCat cells. They show anti-cancer activity towards A431 cells by inducing apoptosis.
40x20mm (600 x 600 DPI)